Arab J Geosci (2016) 9:436
DOI 10.1007/s12517-016-2454-2

ORIGINAL PAPER

# Optimal design of BP algorithm by $ACO_R$ model for groundwater-level forecasting: A case study on Shabestar plain, Iran

Ziba Hosseini[1] · Sajjad Gharechelou[2] · Mohammad Nakhaei[3] · Saeid Gharechelou[4]

Received: 22 June 2015 / Accepted: 30 March 2016


**Abstract** Groundwater always has been considered as one of the major sources of drinking and agricultural water supply, especially in arid and semi-arid zones. Thus, there is a need to simulate (i.e., forecast) groundwater levels with an acceptable accuracy. In this paper, we present two applications of intelligent optimization algorithms for simulations of monthly groundwater levels in an unconfined coastal aquifer sited in the Shabestar plain, Iran. First, the backpropagation neural network (ANN-BP) with seven neurons in its hidden layer is utilized to reproduce groundwater-level variations using the external input variables including the following: rainfall, average discharge, temperature, evaporation, and annual time series. In the next application, ant colony optimization is used to optimize and find initial connection weights and biases of a BP algorithm during the training phase ($ACO_R$-BP). The results were found to be acceptable in terms of accuracy and demonstrated that a hybrid $ACO_R$-BP model is a much more rigorous fitting prediction tool for groundwater-level forecasting. This study has shown that such a hybrid network can be used as viable alternative to physical-based models for simulating the reactions of the aquifer under conceivable future scenarios. In addition, it may be useful for reconstructing long periods of missing historical observations of the influencing variables.

**Keywords** Groundwater level · Unconfined aquifer · Modeling · ANN-BP · Hybrid $ACO_R$-BP

## Introduction

Estimation of groundwater level has a high importance for hydrogeology studies, aquifer management, and agriculture groundwater quality. In many cases, groundwater-level fluctuations have caused irreparable damage on engineering structures. By better understanding the quantities of fluctuations, appropriate decisions can be accessible in terms of water quality, hydrogeology, and management purposes. Although conceptual and physically based models are the main tools for understanding hydrological processes in a basin, these models have some limitations including their requirement of a great quality and quantity of data and their time-consuming processes for simulation. For these reasons, it is very desirable to develop faster and more economical methods for aquifer simulation which can also provide an acceptable accuracy. In order to achieve this goal, many researchers have been using intelligent systems such as artificial neural networks. Among the significant researches can be mentioned to Coulibaly et al. 2001b, 2001c; Lallahem and Mania 2003a, 2003b; Daliakopoulos et al. 2005; Lallahem et al. 2005; Dogan et al. 2008; Nourani et al. 2008; Tsanis et al. 2008; Yang et al. 2009; Sreekanth et al. 2009 and Boucher et al. 2009, which used artificial neural networks for aquifer modeling in diverse basins. A more detailed review of artificial neural network (ANN) applications can be found in Maier and Dandy (2000) and Maier et al. (2010). They reviewed 43 papers which used neural network models for prediction of

✉ Ziba Hosseini
Hosseini@sadi.ut.ac.ir

1 Department of Geology, Faculty of Science, Ferdowsi University of Mashhad, Mashhad, Iran

2 Department of Geology, College of Science, University of Tehran, Tehran, Iran

3 Department of Geology, Faculty of Geoscience, Kharazmi University, Tehran, Iran

4 Department of Arid Land, Semnan University, Semnan, Iran

Published online: 14 May 2016

water resources variables. Some of the studies focused on prediction of groundwater levels by stochastic algorithms method (Chebud and Melesse 2011; Mirzavand and Ghazavi 2014). Moreover, a number of studies compared two or three artificial intelligence methods to find an optimal method for estimation of groundwater levels (Kholghi and Hosseini 2009; Behzad et al. 2010; Shiri and Kisi 2011; Jalalkamali et al. 2011; Shiri et al. 2013; Sahoo and Jha 2013; Fallah-Mehdipour et al. 2013; Maiti and Tiwari 2014; Ying et al. 2014). However, none of the artificial intelligence (AI) methods can dominate other AI methods. In fact, using a hybrid or a multiple AI models for prediction might achieve the optimal performance toward the benefits of all models and avoid bias to a single model (Nadiri et al. 2013).

Giustolisi and Simeone (2006) presented a multi-objective strategy for the optimal design of ANNs when dealing with a nonlinear modeling time series. Moreover, Giustolisi et al. (2008) introduced a modeling approach aimed at the management of groundwater resources based on a hybrid multi-objective paradigm, named Evolutionary Polynomial Regression (EPR). Wang and Zhao (2010) proposed an improved wavelet network model (WNM) which was combined with genetic algorithm (GA) to forecast groundwater level. By comparing it to WNM, their results showed that the GA-WNM predictor can reduce significantly both relative mean errors and root-mean-squared errors of predicted groundwater levels. Chen et al. (2011) and Nourani et al. (2012) evaluated the combination of the backpropagation algorithm and the self-organizing map (SOM) for forecasting the groundwater-level data. According to their study, the SOM-backpropagation (BP) method achieved the highest accuracy. Nourani et al. (2011) used the hybrid of the ANN and geostatistical method for spatiotemporal prediction of groundwater level in a coastal aquifer system. Dash et al. (2010) and Jalalkamali and Jalalkamali (2011) employed a hybrid model of the artificial neural network and genetic algorithm (ANN-GA) for forecasting groundwater level in an individual well. The hybrid ANN-GA was designed to finding an optimal number of neutrons for hidden layer. Furthermore, Hosseini and Nakhaei (2015) presented an application of the hybrid GA-BP model for estimation of groundwater level. The GA has been designed to adjust initial weights of neuron connections and biases for the BP algorithm. The consequences of these researchers admitted the superiority of a hybrid model in the prediction of groundwater level. Adamowski and Chan (2011) proposed a wavelet neural network (WA-ANN) models that provided more accurate forecasts compared to ANN and autoreggresive integrated moving average (ARIMA) models. Moreover, a method combined with discrete wavelet transform method with different mother wavelets and ANN (WANN) was proposed by Nakhaei and Saberi Naser (2012) for prediction of groundwater-level fluctuations in Qurve plain, Iran. In addition, a hybrid model of neuro-fuzzy inference system with wavelet (wavelet-ANFIS) was proposed by Moosavi et al. (2013) for groundwater-level forecasting in different prediction time periods. These studies demonstrated that wavelet transform can improve the accuracy of groundwater-level forecasting. Moosavi et al. (2014) determined the best structures of the wavelet-ANN and the wavelet-ANFIS models for groundwater-level prediction. Their results confirmed that the best wavelet-ANFIS model outperforms the best wavelet-ANN model. Yang et al. (2014) investigated the abilities of WA-ANN and integrated time-series (ITS) techniques to predict the groundwater levels. Their research showed that the WA-ANN computing techniques have better performance than the ITS models. Behnia and Rezaeian (2015) evaluated the coupling wavelet transform with time series models to estimate groundwater levels in two sub-basins in Mashhad plain, Iran. Their results showed that wavelet-SARIMA hybrid model had the better performance than the wavelet-ARMA and the wavelet-ARIMA hybrid model. Raghavendra and Deka (2015) demonstrated the capability of wavelet packet analysis in improving the forecasting efficiency of support vector regression (SVR) through the development of a novel hybrid wavelet packet-support vector regression (WP-SVR) for forecasting monthly groundwater level in three shallow unconfined coastal aquifers located near Mangalore, India. Mirzavand et al. (2015) compared the abilities of two different data-driven methods including the SVR and an adaptive neuro-fuzzy inference system (ANFIS). Their research indicated that the ANFIS model performed better than the optimal SVR model.

The estimation of groundwater-level fluctuation is commonly carried out by means of well-known numerical models such as MODFLOW, USGS, which claim an appropriate synthesis of the aquifer parameters to describe the spatial variability of the subsurface. The required data for this model is hard to obtain even with expensive site investigations and generally results in extreme computational costs. Although, developing a rigorous numerical model of the flow system is preferable, as it entails a deeper understanding of the aquifer system dynamics (Taormina et al. 2012), but according to the results of new hybrid intelligent optimization methods, there is an appropriate method with an acceptable range of error as a good alternative. Among the intelligent methods, $ACO_R$ is the newest method that is used for high-performance modeling in the field of hydrology. The study processes emphasize the importance of using a hybrid AI model for groundwater-level prediction rather than a single AI model. The background review of this paper obviously showed the backpropagation algorithm is the most popular in the domain of neural networks which is utilized in the most of the mentioned studies for aquifer simulation. The contribution of this study first estimation of groundwater level would be illustrated using a BP neural network that is called the ANN-BP. The BP is the standard of gradient descent algorithm, and this method is easily getting stuck in a local minimum and often needing longer training time (Chau 2007). Hence, in the next method, the stochastic optimization method ($ACO_R$) is utilized to train a feed-forward neural network; therefore, numerical weights of neuron connections and biases represent the solution components of the optimization problem. The $ACO_R$ is one type of stochastic algorithms that are capable of solving multi-dimensional complex problems especially non-smooth, non-continuous, non-differentiable objective function to find the global optimum, to escape the local optima and acquire a global optimal solution.

$ACO_R$ in comparison to other stochastic algorithms has a powerful memory that keeps a history of all iterations. So, its probability distribution depends on each iteration and defines by a Gaussian kernel function. The Gaussian kernel function is as a weighted sum of several one-dimensional Gaussian functions. It allows a reasonably easy sampling and yet provides a much-increased flexibility in the possible shape, in comparison to a single Gaussian function. These properties of the $ACO_R$ are causing better exploration and the more acceptable results than other algorithms as API, CACO, CACS, and CIAC (Socha 2008).

The combination of $ACO_R$ and BP would be an efficient method of training neural networks, because it takes advantage of the strengths of ant colony algorithm and backpropagation (the fast initial convergence of stochastic algorithms and the powerful local search of backpropagation), and overcomes the weaknesses of the two methods (the weak fine tuning capability of stochastic algorithms and a flat spot in backpropagation). After the performance of a hybrid model and an ANN-BP model, this study will present estimation of groundwater level in an unconfined coastal aquifer.

## Study area and data

The data used in this study are from the Shabestar plain (Fig. 1) which is located in the northwest of Iran at East-Azerbaijan province. It is between 45° 26′ and 46° 2′ north latitude and 38° 3′ and 38° 23′ east longitude with arid and cold climate. The plain area is about 1297 $km^2$, and its main river is Daryanchai. The headwaters of the river are situated in height about 2982 m of the Misho Mountain, and it discharges into Urmia Lake. According to statistical results of 40 recent year's data, average discharge of Daryanchai River has been 0.475 $m^3/s$. The mean daily temperature varies from −19 °C in January up to 42 °C in July with a yearly average of 11 °C, and the average annual rainfall is about 250 mm (Nourani and Ejlali 2012).

As showed in Fig. 1, the study area is a coastal aquifer system. Coastal areas are very important for human settlement and development (Datta et al. 2009). A lot of populations are living in Urmia Lake basin, whose economic irrigation is strongly dependent on the existing surface and groundwater resources in the area. Accordingly, the focus of the human population, the indiscriminate use, and the recent drought have reduced the lake water level and seasonal main river. Therefore, in recent years, groundwater is a major source of drinking and agricultural water supply.

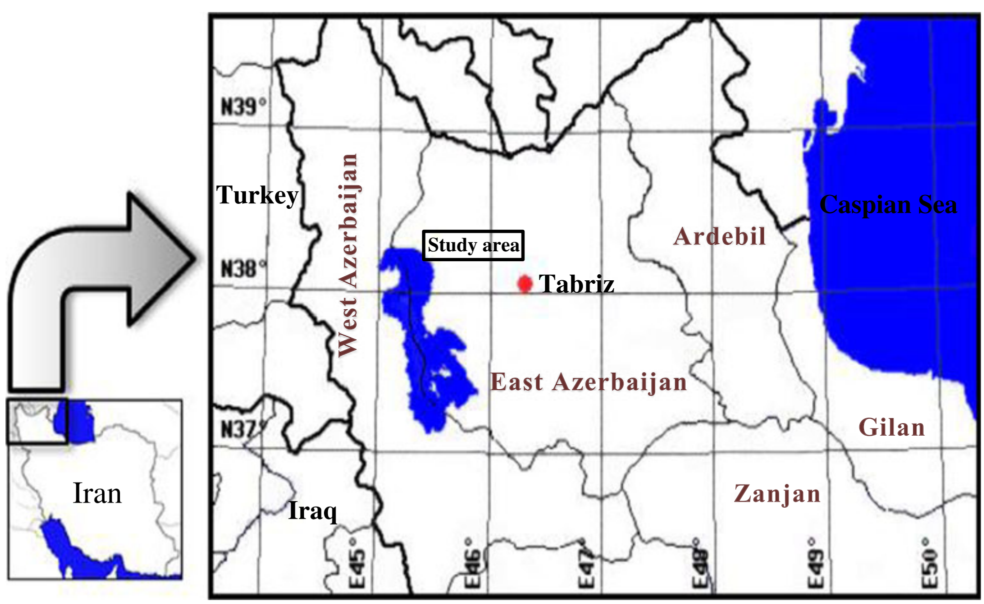


**Fig. 1** Study area in northwest of Iran

## Geological and hydrogeological framework

The Shabestar plain in NW of Iran is composed of Quaternary sediments. These sediments include conglomerate, sandstone, clay, and limestone. Rarely in upper layers of the aquifer are evaporite sediments besides marls as an interlayer. Clastic sediments (conglomerate and sandstone) in this plain are well sorted that resulted in porous aquifer. Geological map of the plain and 15 selective piezometers in the aquifer are shown in Fig. 2.

The elevation of the northern part of the aquifer is higher, and the general slope of the plain is from north to south. The northern part of the plain is composed of coarse and well-sorted sediment with high permeability and low thickness, and the southern part of the plain contains fine sediments which are not suitable for groundwater storage. Moderately sandstone grain with high thickness is in the southwest and east part of the plain due to profitable (permeable) aquifer with resistivity of about 20 to 60 Ω-meter.

The bedrock of the aquifer is Miocene marl and clayey formations. These fine and clayey sediments are barriers versus salt water invasion from the lake. This aquifer in the most sectors of the studied area is unconfined because of low thickness of the impermeable layer, discontinuity, and low specific resistance.

Figure 3 shows the groundwater-level distribution in 2009. Groundwater flow direction in the Shabestar plain aquifer is mainly from north to south. However, in some parts of the plain because of the high number of pumping wells, flow direction is locally out of the main flow trend in the plain and changed to the closed water table contours.

## Methods

### Artificial neural network

Neural networks are basically composed of interconnected simulated neurons. Nowadays, in hydrological engineering application, widely using network is the feed-forward neural network (FF-NN). This is largely due to its simplicity compared to other networks and its ability to learn the implicit governing relation between the inputs and outputs if sufficient training data is supplied. The FF-NN is a network structure in which the information or signals will propagate only in one direction. The FF-NN typically consists of three layers including input, hidden, and output layers, which are depicted in Fig. 4. It is possible to have more than one hidden layer, but a single layer is sufficient to approximate any function to a desired degree of accuracy (Hornik et al. 1989). The number

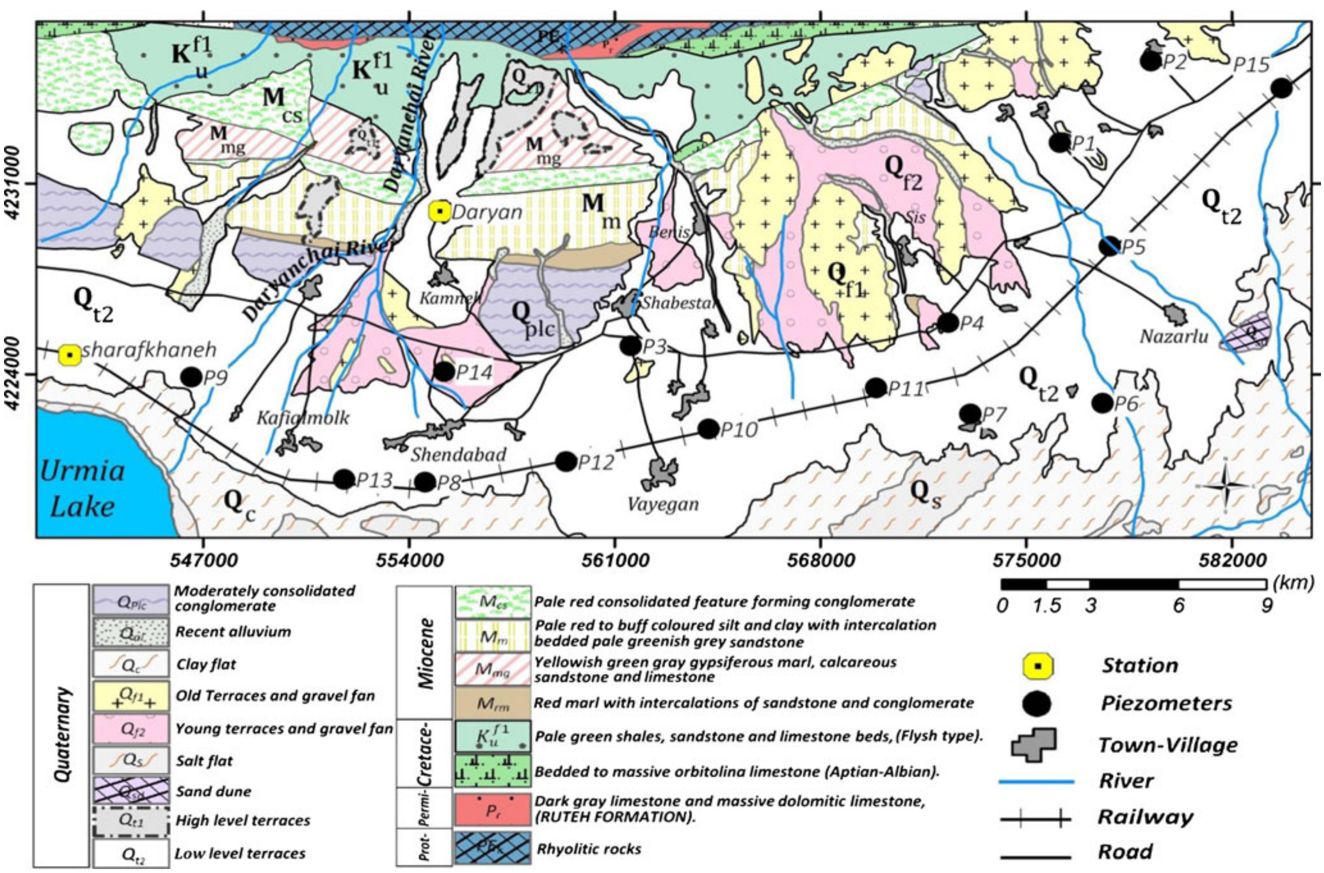

**Fig. 2** Geologic map and piezometer position in the Shabestar plain (base geological map: Asadian et al. 2007)

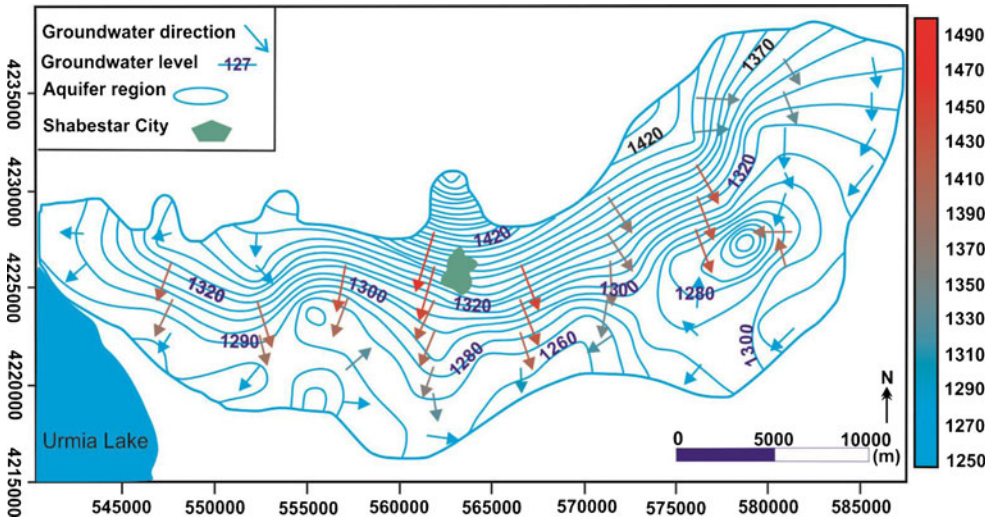


**Fig. 3** Groundwater level and flow direction of study area (June 2009)

of neurons in the input and output layers is normally determined by the special problem. As well for most cases, the best way to determine the optimal number of neurons in the hidden layer is done by systemic trial-and-error method. In fact, the inputs are fed through the input layer and, after being multiplied by synaptic weights, are delivered to the hidden layer. In the hidden neurons, the weighted sum of inputs is transformed by a nonlinear activation function, which is usually chosen as the logistic or the hyperbolic tangent. The same process earnings place in each of the following hidden layers, until the outcomes reach the output neuron. Meanwhile, the linear activation function is most commonly applied to output layer (Triana et al. 2010).

BP algorithms are the most popular training algorithms that are widely used due to their simplicity and the application for training FF-NN (Kulluk 2013). In the FF-BP networks, which are considered in this study, output error is reported back, and in this way, a more desirable output is acquired through updating weighting coefficient matrix. This action is carried out until the error between the target data and output data derived from the weighing matrix is insignificant, and consequently, a value of the objective function is minimized. For further details on the FF-NNs, the reader is referred to the bibliography (ASCE Task Committee on Application of Artificial Neural Networks in Hydrology 2000) and Dawson and Wilby (2001).

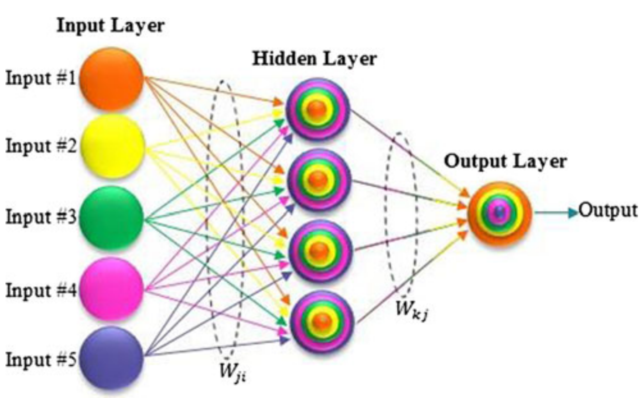


**Fig. 4** Typical feed-forward neural networks

## Hybrid $ACO_R$-BP model

The combination of $ACO_R$ and BP algorithms can lead to an increase in speed and accuracy of presenting the most optimum results because the $ACO_R$ algorithm, considering its exploratory characteristics, is applied for training a neural network which itself is capable of extracting solutions. Therefore, the primary adjustment of weighting coefficients of neuron connections is done by $ACO_R$ and the final optimization is done by neural network itself. In other words, the $ACO_R$-BP model (Socha and Blum 2007) which is designed in this study is a hybrid optimization algorithm that uses $ACO_R$ in the training phase of a feed-forward BP neural network.

In recent years, a combination of $ACO_R$ and BP is designed for optimization of different problems. Some of these algorithms are used in oil and gas engineering modeling (Ashena and Moghadasi 2011; Tabatabaei et al. 2015; Safarvand et al. 2015; Kia et al. 2015). Also, this algorithm is applied for pattern classification (Mavrovouniotis and Yang 2014), thermal anomaly detection prior to earthquakes (Choubsaz et al. 2015), and automobile automatic transmission shift control (Chen and Yu 2012). This research particularly shows a combination of BP and $ACO_R$ in groundwater-level forecasting and water resource management.

$ACO_R$ algorithm is one of the ACO categories that were presented for its compatibility with continuous search space without substantial change in its main algorithm (Socha and Dorigo 2008). The $ACO_R$ algorithm holds $k$ best solutions in a matrix $T_{k \times n}$ that called solution archive ($n$ is the dimension of the optimization problem). The main goal of creation this matrix is to define a probability distribution over the search domain. On the other hand, each solution represents the center of a different Gaussian PDF (probability density function). In the first step of implementation of the algorithm, all points in the search space have an equal probability of being selected by using a uniform distribution probability. For each dimension, a Gaussian kernel as a weighted sum of several one-dimensional Gaussian functions ($g_l^i$) was defined and it is given by Eq. 1:

$$G^i(x) = \sum_{l=1}^{k} w_l g_l^i(x) = \sum_{l=1}^{k} w_l \frac{1}{\sigma_l^i\sqrt{2\pi}} e^{-\frac{\left(x-x_l^i\right)^2}{2\sigma_l^{i\,2}}} \tag{1}$$

where $l \in \{1, \dots, k\}$ , $i \in \{1, \dots, n\}$ and $n$ is the problem dimension and $k$ is the number of the best solutions in solution archive. $x_l^i$ is the $l$th solution of $i$th dimension in solution archive.

$w_l$ is the weight that is assigned to each solution based on its rank (from best to worst). $w_l$ is calculated according to Eq. 2:

$$w_l = \frac{1}{\sqrt{2\pi\mathrm{qk}}} e^{\frac{-(r_l-1)^2}{q^2k^2}} \tag{2}$$

The value of ($r_l$ = 1,2,…, $k$) is the rank of solutions in the solution archive. The lower and upper limits of $w_l$ are changes with $q$ parameter. When $q$ is small, the best-ranked solutions are strongly preferred (Socha and Dorigo 2008). The elements of the weight vector $x$ are computed by Eq. 3. Then, the sampling is completed in two phases. The first phase consists of choosing one of the Gaussian functions that composes the Gaussian kernel PDF. The probability of choosing the $l$th Gaussian function is given by the following:

$$p_l = \frac{w_l{}^l}{\sum_{r=1}^{k} w_r{}^r} \tag{3}$$

The second phase consists of sampling the chosen Gaussian function. This may be done by using a random number generator that is able to generate random numbers according to a parameterized normal distribution.

Sigma is the standard deviation of normal distribution PDF, which is calculated in Eq. 4:

$$\sigma_l^i = max\left\{\frac{max\left(x_{1,\dots,k}^i\right)-min\left(x_{1,\dots,k}^i\right)}{u.w_l.\sqrt{t}}, \varepsilon\right\} \tag{4}$$

where $t$ represents the iteration and $k$ is the number of the solution in solution archive. $u$ is a parameter for adjusting the speed of convergence. The lower limit is considered for the value of $\sigma$ by using $\varepsilon$.

In each iteration, the $\mathrm{ACO_R}$ algorithm refines and regenerates the solution archive by adding $m$ new solutions ($k \rightarrow k + m$) and then eliminates worst $m$ solutions ($k + m \rightarrow k$) in order to keep the size of the solution archive constant (negative and positive update). As results of the change in solutions stored in the solution archive, each iteration pheromone is increased in optimized paths that have not an improvement in the objective function. In this way, the best solution for the problem is found through the $\mathrm{ACO_R}$ algorithm. After that, this procedure is completed by applying a BP training algorithm on $\mathrm{ACO_R}$ established initial connection weights and biases (Fig. 5).

## Application to the Shabestar plain

### Observed data

The predictive ability of intelligent systems depends heavily on the choice of the input set, which should ideally contain only variables with explanatory potential. This issue is particularly critical when employing hybrid or individual FNNs for time series applications since time-lagged autoregressive and exogenous inputs must be explicitly provided to explain the behavior of dynamical systems (Maier and Dandy 2000). According to the result of the recent researches (Coulibaly et al. 2001a; Lallahem et al. 2005; Nourani et al. 2008), effective factors that are in fluctuation of groundwater level are temperature, rainfall, and an average discharge of basin. But, typical hydrology and hydrogeology of every basin are

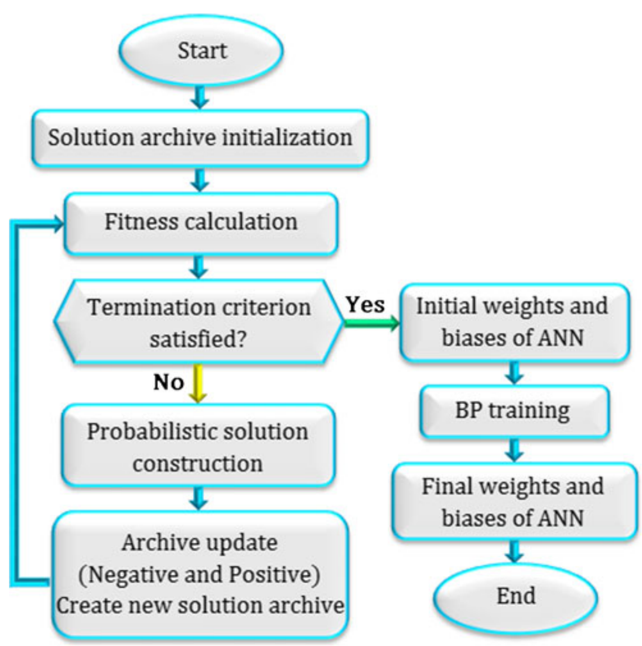


**Fig. 5** $\mathrm{ACO_R}$-BP flow chart (Tabatabaei et al. 2015)

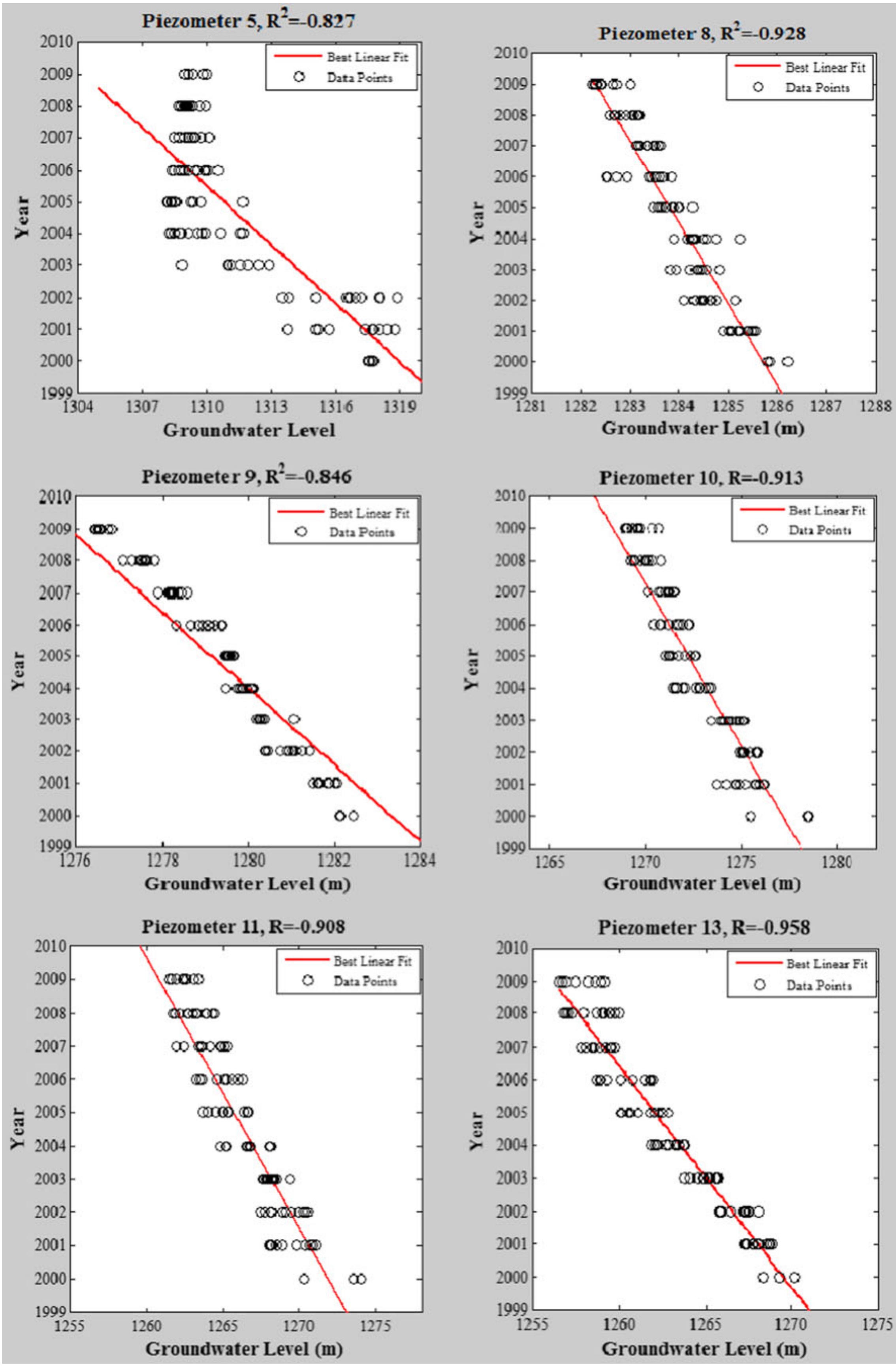


**Fig. 6** Cross-plots showing relationship between groundwater level and annual time series in six piezometers

different. Therefore, input data trending should be considered in an aquifer modeling. The groundwater level in Shabestar plain aquifer was decreasing in all piezometers. Undoubtedly, evaporation also is an important factor in groundwater-level depletion. Therefore, the evaporation data were added to the input parameters. Similarly in another case study, evaporation factor is used for estimation of groundwater level in other coastal aquifer sited in Italy (Taormina et al. 2012). These four input data (temperature, rainfall, average discharge, and evaporation) reflect monthly fluctuations in the groundwater level since piezometer groundwater-level decrease with constant gradient annually; annual time series are also included for the present study.

The annual time series has entered with the number of the year and statistically has a good linear relation with the groundwater level. Derived regressions show more than 80 % of the correlation coefficient in six piezometers (Fig. 6). Therefore, checking this parameter in aquifers which annually have decreased or increased in groundwater level can be useful in designing simulating network.

For this purpose, the data were collected for 9 years (from October, 2000, to September, 2009) with 1-month time interval. The monthly data utilized consist of the following categories:

1. Observed groundwater level at 15 piezometers (m)

The statistical analysis of the observed groundwater levels is shown in Table 1 for selected piezometers. Correspondingly, Fig. 2 shows positions of the piezometers located within the Shabestar plain. The chosen piezometers were selected based on the uniform distribution in the plain, completeness of the data category, and far enough distance from the coastal line.

2. Rainfall (mm/month) in Sharafkhaneh station
3. Average discharge of Daryanchai river ($m^3/s$) in Daryan station
4. Evaporation (mm/month) in Sharafkhaneh station
5. Temperature (°C) in Sharafkhaneh station
6. Annual time series (year)

Rainfall value ranged is from 3 to 110.2 mm/month (average 20.39), average discharge value is from 0.03 to 2.658 $m^3/s$ (average 0.41), temperature value is from −6.7 to 27 °C (average 13.41), and evaporation value is from 0 to 265.9 mm/month (average 87.39).

Toward the achieving better assessment of the results, all input and output data were normalized using introduced method by Larose in data mining and statistical analysis (Larose 2005). Normalization is performed according to Eq. 5 in the typical range of 0 (L) and 1 (H) by using the maximum and minimum values:

$$X^* = mX_i - b \tag{5}$$

$$m = \frac{H-L}{\mathrm{Max}\,(X) - \mathrm{Min}\,(X)} \tag{6}$$

$$b = \frac{\mathrm{Max}\,(X)L + \mathrm{Min}(X)H}{\mathrm{Max}(X) - \mathrm{Min}\,(X)} \tag{7}$$

where $X^*$ is the normalized variable and $X_i$ is the main variable.

**Table 1** Statistical analysis of observed groundwater in 15 piezometers

| Piez. no. | *X* (UTM) (m) | *Y* (UTM) (m) | Mean (m) | Min (m) | Max (m) | Variance | Standard deviation(m) | Skewness coefficient |
|---|---|---|---|---|---|---|---|---|
| P1 | 576,150 | 4,232,500 | 1412.45 | 1408.31 | 1415.95 | 2.274615 | 1.508182 | −0.047228 |
| P2 | 579,250 | 4,235,500 | 1363.58 | 1362.74 | 1365.67 | 0.407335 | 0.638228 | 0.778455 |
| P3 | 561,550 | 4,225,050 | 1334.10 | 1331.19 | 1357.68 | 7.269294 | 2.696162 | 6.299276 |
| P4 | 572,350 | 4,225,900 | 1329.07 | 1322.81 | 1336.86 | 25.60608 | 5.060245 | 0.168759 |
| P5 | 577,850 | 4,228,700 | 1311.56 | 1304.93 | 1318.91 | 12.27430 | 3.503471 | 0.880152 |
| P6 | 577,600 | 4,222,950 | 1298.84 | 1292.96 | 1300.16 | 0.632857 | 0.795523 | −3.637452 |
| P7 | 573,100 | 4,222,550 | 1294.82 | 1292.31 | 1296.01 | 0.547359 | 0.739837 | −0.491028 |
| P8 | 554,550 | 4,220,050 | 1283.90 | 1282.23 | 1286.22 | 0.871312 | 0.933441 | 0.152471 |
| P9 | 546,600 | 4,223,900 | 1279.37 | 1269.56 | 1282.44 | 3.421868 | 1.849829 | −1.393301 |
| P10 | 564,200 | 4,222,000 | 1272.48 | 1265.55 | 1278.54 | 5.590902 | 2.364509 | 0.170974 |
| P11 | 569,900 | 4,223,500 | 1266.02 | 1259.51 | 1274.08 | 8.643071 | 2.939910 | 0.276150 |
| P12 | 559,350 | 4,220,800 | 1260.85 | 1257.32 | 1266.72 | 3.440292 | 1.854802 | 0.284084 |
| P13 | 551,800 | 4,220,150 | 1262.46 | 1256.44 | 1270.23 | 14.251235 | 3.775080 | 0.246874 |
| P14 | 555,200 | 4,224,100 | 1254.83 | 1250.83 | 1264.02 | 7.935692 | 2.817036 | 1.230776 |
| P15 | 583,700 | 4,234,500 | 1329.79 | 1328.99 | 1331.91 | 0.270965 | 0.520543 | 1.158132 |

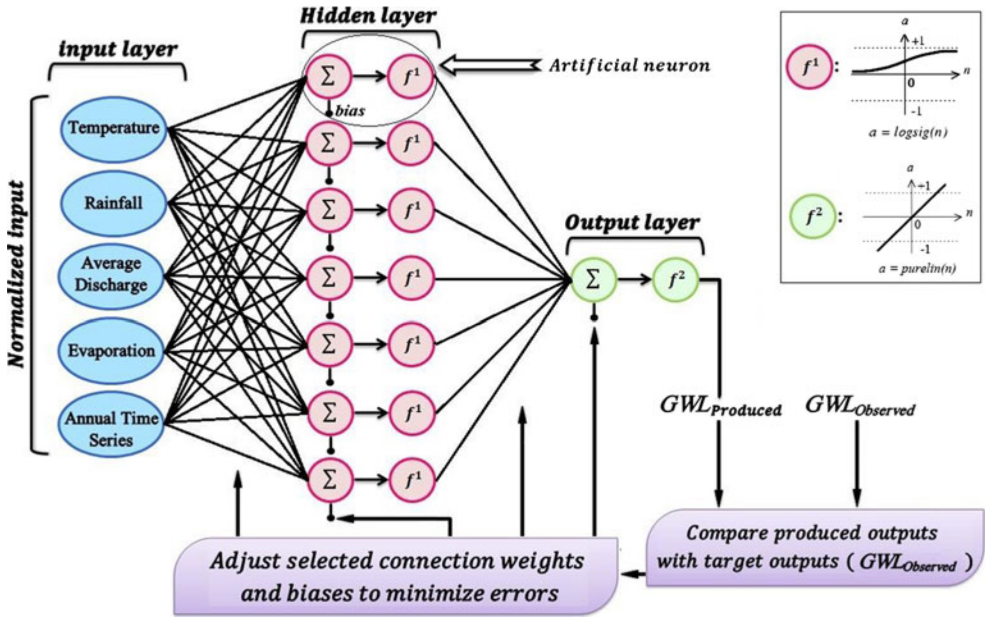


**Fig. 7** Typical architecture of feed-forward BP neural network with seven neurons in hidden layer by comparing produced groundwater level ($WL_{\text{produced}}$) and observed groundwater level ($WL_{\text{observed}}$) during the training phase; errors propagate backward to the connections in the previous layers

## Applied artificial neural network structure

The structure of the ANN-BP was designed (5:7:1) for both models, consisting of three layers including an input layer, a hidden layer, and an output layer as shown in Fig. 7. The architecture of feed-forward BP neural network consists of five input variables, seven hidden neurons with logistic function and one output variable with linear activation function transforming the sum of all the weighted inputs into an output signal. By using a trial-and-error method, it was realized that a structure with seven neurons in the hidden layer (5:7:1 structure) gives the best results.

**Table 2** Parameters used in construction of $ACO_R$-BP model

| $ACO_R$-BP properties | Properties |
|---|---|
| Probability density function | Gaussian kernel PDF (Eq. 1) |
| $m$ | 200 |
| $k$ | 10 |
| $u$ | 10 |
| $q$ | 0.5 |
| $\varepsilon$ | 0.0005 |
| $ACO_R$ maximum of iterations | 50 |
| Type of neural network | FF-BP |
| Number of layer in neural network | 3 |
| Number of neurons in hidden layer | 7 |
| Transfer function from layer 1 to 2 | LOGSIG |
| Transfer function from layer 2 to 3 | PURELIN |
| BP maximum of epoch | 100 |

The trial-and-error method was examined with the great scale of the neuron for both ANN and $ACO_R$ networks. The experimental results indicate that with increasing the number of neurons in the hidden layer, the function of $ACO_R$ in discovering the primary coefficients will slowdown. Besides, the conclusions of the hybrid network were similar for the vast range of neurons which makes it too difficult for selecting the number of neurons through the $ACO_R$-BP. As a result, the decision to choose the number of neurons is taken only based on the results of ANN-BP in the range of 3 to 12 neurons which the best result in most of the piezometers was seven neurons in the hidden layer.

## Optimization of weight connections using hybrid $ACO_R$-BP

In this study, the hybrid model of $ACO_R$-BP is designed in comparison with the ANN-BP for estimation of groundwater level. For this purpose, the weight adjustment is done by minimizing the objective function which is normally defined as root-mean-squared error (RMSE) which calculates according to the following formula:

$$\text{RMSE} = \sqrt{{}^{1}/_{N}\sum_{i=1}^{N}\left(WL_{\text{observed}}-WL_{\text{predicted}}\right)^{2}} \quad (8)$$

In this equation, RMSE is the root-mean-squared error, $N$ is the number of training samples, $WL_{\text{obseved}}$ is the amount of observed groundwater level for each piezometer, and $WL_{\text{predicted}}$ is the predicted amount of groundwater level using ANN-BP or $ACO_R$-BP.

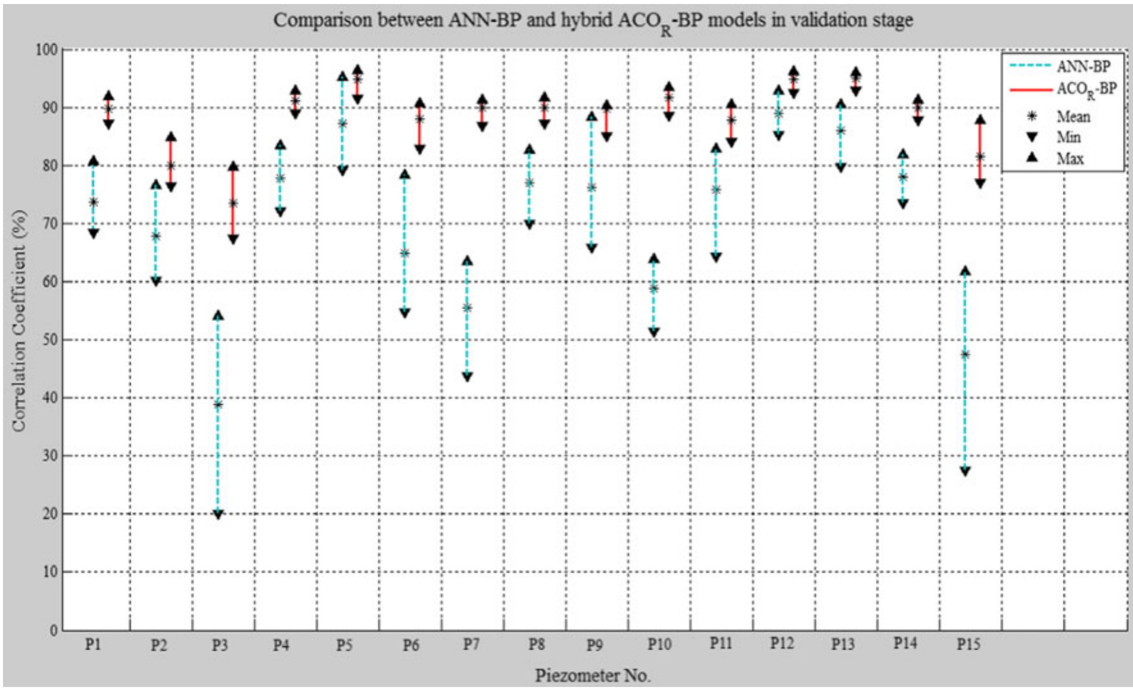


**Fig. 8** Validation results from simulation of groundwater level by 30 times model run

The coding model is done in MATLAB software (version 2014) environment. Table 2 represents that the parameters were used in the construction of the ACO$_R$-BP model. The detailed algorithm of hybrid neural network-ACO$_R$ designed in this study to find weights and biases is as follows. Consideration of groundwater level is estimated from predefined inputs by using Eq. (9).

$$WL^{\text{predicted}}_{1\times1} = LW_{1\times7} \times \text{Tansig}(IW_{7\times5} \times P_{5\times1} + b_{7\times1}) + d_{1\times1} \tag{9}$$

In Eq. (9), $LW$ and $IW$ are unknown weight matrices and $b$ and $d$ are unknown biases that should be computed. For seven neurons in hidden layer, the total number of unknown variable is $n = (1 \times 7) + (7 \times 5) + (7 \times 1) + (1 \times 1) = 50$. The detailed algorithm of ACO$_R$ to find weights and biases is as follows:

1. Read input data $P_{5\times1}$ for $N$ sample.
2. Select $S$, the number of neurons in hidden layer ($S = 7$).
3. Compute $n$, the number of unknown weight and bias values (according to Eq. (9), $n = S \times (\text{length}(p) + 2) + 1 = 50$).
4. Select $k$, the number of the solutions is stored in solution archive matrix. $T_{k\times n}$ (each row in the solution archive matrix corresponds to a found solution).
5. Initialize solution archive matrix ($T_{k\times n}$) with $k$ random solutions.

For $i = 1$ to max_iter do

1. Compute $WL^{\text{predicted}}$, according to Eq. (9).
2. For each solution $x_l$ in the solution archive matrix, the value of the objective function $f(x_l) = RMSE(x_l)$ Eq. (8) is calculated according to Fig. 5.
3. Sort the solutions in the solution archive matrix according to their objective value ($f(x_1) < f(x_2) < \ldots < f(x_k)$), where $k$ is the number of rows (solutions)
4. Calculate the weight of $w$, which is $w_1 > w_2 > \ldots > w_k$, according to Eq. (2),
5. Compute the probability of the roulette wheel $p_i$, according to Eq. (3)
6. Repeat the following steps, $m$ times to generate $m$ new solutions: produce a new value repeatedly for each variable of a new solution by employing the normal distribution $g_l^i(x) = \frac{1}{\sigma_l^i\sqrt{2\pi}} e^{\frac{-(x-x_l^i)^2}{2\sigma_l^{i2}}}$ where $x_l^i$ is a value selected from the $i^{\text{th}}$ value (variable) of the $i^{\text{th}}$ solution in the solution archive matrix by the probability of $p_i$, and $\sigma_l^i$ is defined as Eq.(4).
7. Adding these $m$ new solutions ($k \to k + m$) to the solution archive matrix and then eliminate worst $m$ solutions ($k + m \to k$) in order to keep the size of the solution archive constant (positive and negative update).
8. The first row of the solution archive matrix is the best weights and biases that are found by ACO$_R$.

**Table 3** The results of models for estimation of normal groundwater level

| Piez. no. | $ACO_R$-BP | | | | | | ANN-BP | | | | |
|---|---|---|---|---|---|---|---|---|---|---|---|
| | Training | | Test | | Validation | | Training | | Test | | Validation |
| | RMSE (cm) | $R^2$ (%) | RMSE (cm) | $R^2$ (%) | RMSE (cm) | $R^2$ (%) | RMSE (cm) | $R^2$ (%) | RMSE (cm) | $R^2$ (%) | RMSE (cm) |
| P1 | 11.7 | 98.1 | 12.1 | 91.6 | 11.8 | 91.8 | 16.6 | 97.1 | 18.7 | 82.3 | 19.1 |
| P2 | 7.6 | 98.9 | 8 | 90.7 | 9.1 | 84.8 | 9.5 | 97.5 | 12.1 | 75.4 | 12.9 |
| P3 | 9.5 | 99.3 | 10.3 | 89.8 | 14.7 | 79.7 | 12.9 | 98.3 | 15.4 | 47.6 | 14.8 |
| P4 | 10.9 | 99.2 | 11.5 | 97.5 | 12.4 | 92.8 | 15.4 | 97.4 | 17.6 | 88.1 | 18.6 |
| P5 | 11.2 | 99.5 | 11.4 | 91.2 | 11.6 | 96.3 | 13.9 | 97.6 | 17.7 | 68.9 | 15.3 |
| P6 | 12.8 | 98.7 | 13.7 | 90.1 | 13.9 | 90.7 | 17.1 | 92.6 | 19.4 | 76.8 | 20.2 |
| P7 | 10.4 | 98.1 | 12.4 | 92.5 | 14 | 91.2 | 16.9 | 95.9 | 19.2 | 79.1 | 18.7 |
| P8 | 9.2 | 98.9 | 10.5 | 92.9 | 10.1 | 91.6 | 13.9 | 97.3 | 16.5 | 84.8 | 15.4 |
| P9 | 8.7 | 99.2 | 9.8 | 91.7 | 10.3 | 90.4 | 14.1 | 98 | 19.3 | 84.2 | 18.1 |
| P10 | 10.3 | 98.5 | 12.2 | 89.6 | 11.8 | 93.4 | 12.3 | 95.7 | 15.8 | 78.2 | 17.5 |
| P11 | 12.9 | 99.1 | 13.5 | 91.3 | 13.7 | 90.6 | 16.3 | 96.9 | 18.9 | 87.1 | 20 |
| P12 | 11.1 | 98.3 | 11.6 | 97.5 | 12.4 | 96.2 | 15.4 | 94.3 | 17.4 | 92.6 | 17.3 |
| P13 | 10.6 | 99.4 | 10.9 | 96.1 | 10.6 | 95.9 | 12.8 | 98.7 | 14.1 | 92.1 | 14.3 |
| P14 | 12.1 | 98.2 | 12.9 | 92.6 | 13.2 | 91.2 | 16.1 | 95.4 | 22.3 | 83.3 | 20.1 |
| P15 | 7.1 | 97.3 | 8.6 | 89.7 | 7.9 | 87.8 | 10 | 95.2 | 10.6 | 67.4 | 11.4 |

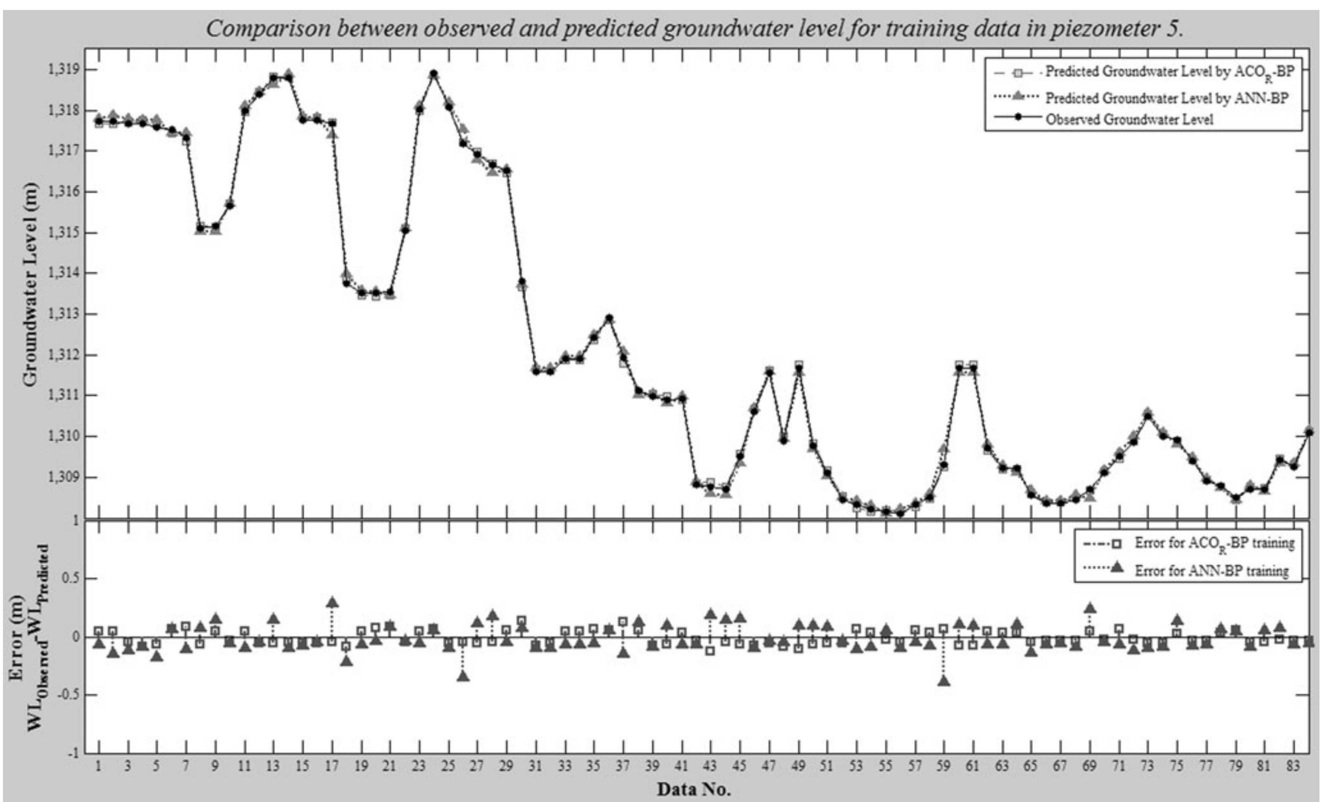


**Fig. 9** Graphical comparison of estimated versus observed groundwater level at piezometer P5 using $ACO_R$-BP and ANN-BP in training step

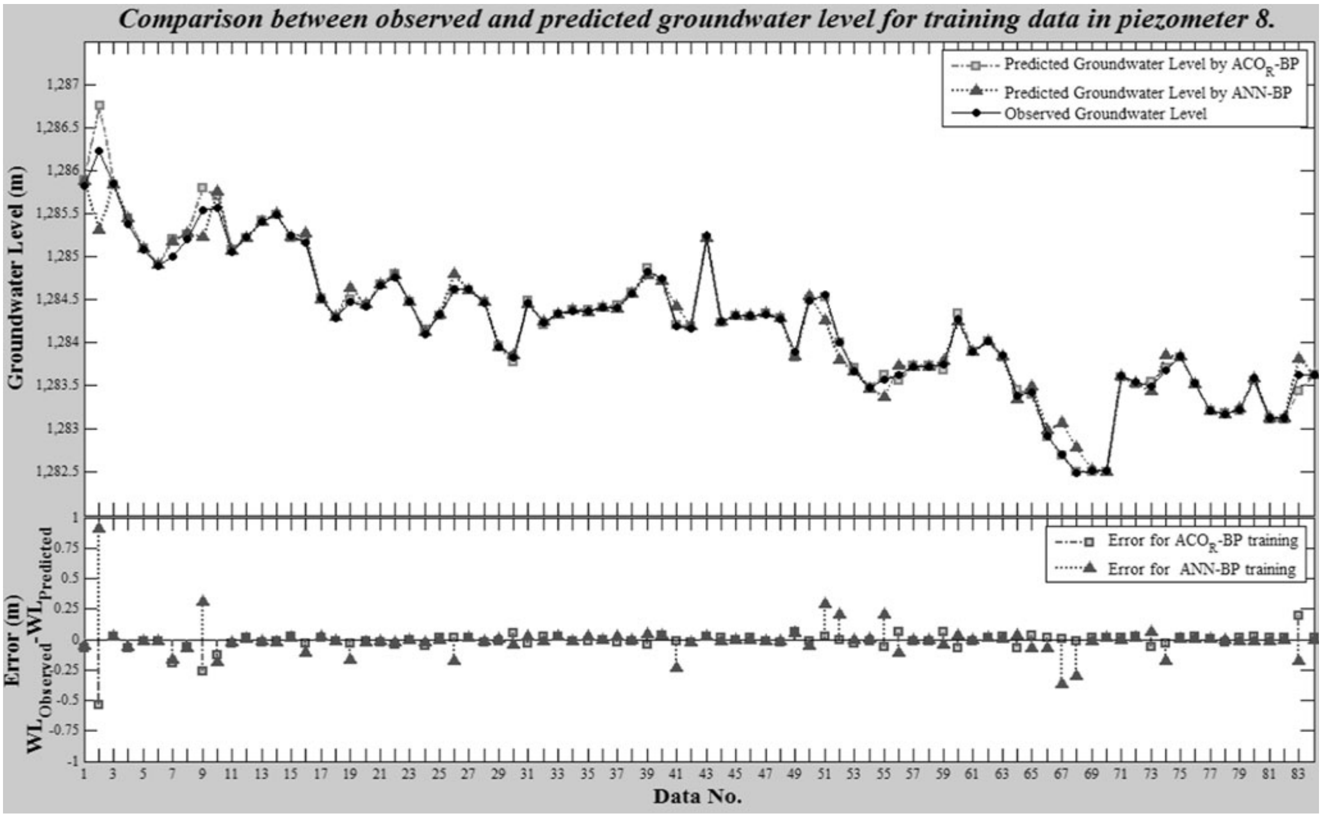


**Fig. 10** Graphical comparison of estimated versus observed groundwater level at piezometer P8 using ACO$_R$-BP and ANN-BP in training step

## Results and discussion

To approach an appropriate comparison between the different intelligent optimization methods, the same set of input/output data and training, testing, and validation set were used. Meanwhile, it is tried to use the same parameter setting for the individual and hybrid model. The total dataset includes 84 training data for each piezometer (October 2000 to September 2007), 12 testing data (October 2007 to September 2008), and 12 validation data (October 2008 to September 2009) used for validation. To validate the accuracy, RMSE and correlation coefficients ($R^2$) were calculated between observed and estimated data.

For accurate evaluation, two methods (ANN-BP and ACO$_R$-BP) for estimation of groundwater level were run for 30 times. The results of each run time of the models and comparison of the minimum, mean, and maximum correlation coefficients are shown in Fig. 8. The diversity of results to some extent of 15 piezometers shows that single neural network has higher scattering than hybrid model.

In overall, an $R^2$ value greater than 90 % indicates a very satisfactory model performance, while an $R^2$ value in the range of 80–90 % signifies a good performance, and the value less than 80 % indicates an unsatisfactory model performance (Coulibaly and Baldwin 2005). Thus, the hybrid net (ACO$_R$-BP) indicates the better results in the validation. Table 3 shows the most optimal results from models in each step of training, test, and validation. At results, the table is gain from the estimation of groundwater level that in each run of the hybrid model achieved a lower data distribution and better results of the most optimal model in each data class.

According to Table 3, ACO$_R$-BP has the best performance in training step and has achieved the best results for test and validation data. The average $R^2$ of testing and validation for ACO$_R$-BP model set has been more than 90 %. Also, this model is faster than the ANN-BP model. The results of the Table 3 indicate that the individual neuron network with the past 7-year training has no flexibility to the new changes in the last 2 years. This network only works out well for the two piezometers of 12 or 13 because the monthly data tests and the validation trend are similar to the training one in piezometers. For instance, continuously in 6 years from September to October, the water table was 1261 m; it means that the change was not that considerable. Overall, for the half of the piezometers (P2, P3, P5, P6, P7, P10, P15), the neural network individually shows less than 0.8 correlation coefficient in testing stage and validation, which the function is not appropriate in the present research and the training network does not have the flexibility to predict the necessary changes. Using of ACO$_R$ algorithm for escaping the local optimization and training accurately, the neural network causes to explore the hybrid network of ACO$_R$-BP with the better quality or flexibility for predicting the extrapolation issues. This system works the best in most piezometers, and the correlation coefficient in data test and validation is more than 0.9. On the other hand, according to the results of Table 3, the hybrid network in piezometers P2, P3, and P15 also does not indicate a very good performance.

Although hybrid net in piezometer 3 has higher performance than the individual neural network, both nets concordant in the estimation of test and validation correlation coefficient are lower than 0.8. In the piezometer 3, a difference of groundwater level in 7 years of training data is 26.49 m while, in the last 2 years, it was 1.77 m. Probably, a high difference of groundwater level in training data against the test and validation data is the most cause of reducing the c in the hybrid $ACO_R$-BP. Moreover, Fig. 2 shows that piezometer 3 is near Shabestar city. In fact, high pumping area near the city is causing greater groundwater-level reduction.

In the piezometers P2 and P15, groundwater levels have been changed only 2 cm from January to June 2009. Fixation of groundwater level in six consecutive months with consideration to frequent changes in input variables, such as precipitation, has been the main reason for low correlation coefficient in validation stage. Probably, observation groundwater level was not measured accurately for piezometers P2 and P15 in 2009. Therefore, the validation result of these two piezometers cannot determine the reliability of network accuracy. In the testing stage, the correlation coefficient is calculated about 90 % for these two piezometers. So, without considering validation data, it can realize that hybrid $ACO_R$-BP was appropriated in these two piezometers. The results of network training with error value for piezometers P5 and P8 are shown in Figs. 9 and 10.

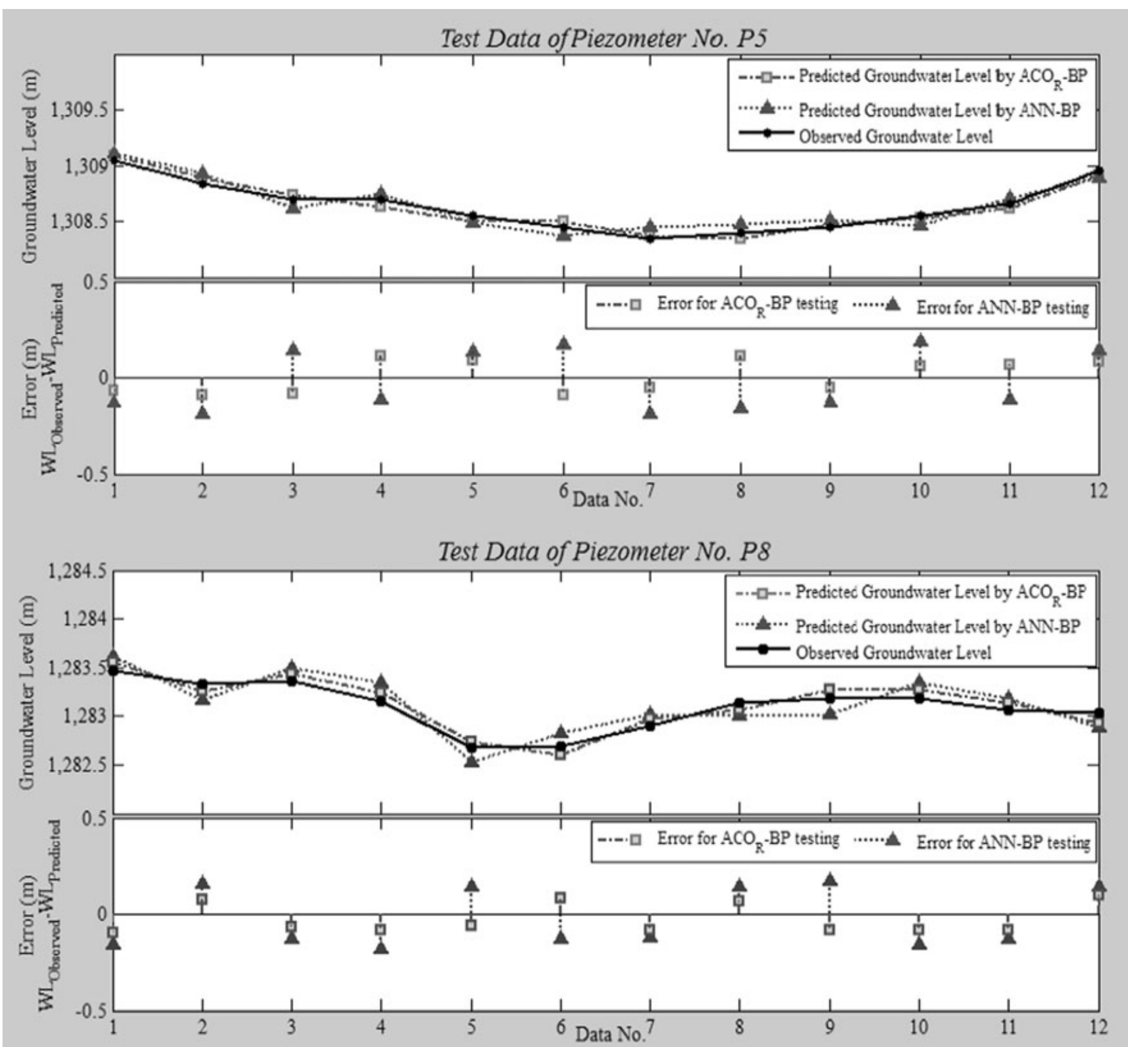


**Fig. 11** Graphical comparison of estimated versus observed groundwater level at two selected piezometers using $ACO_R$-BP and ANN-BP in test step

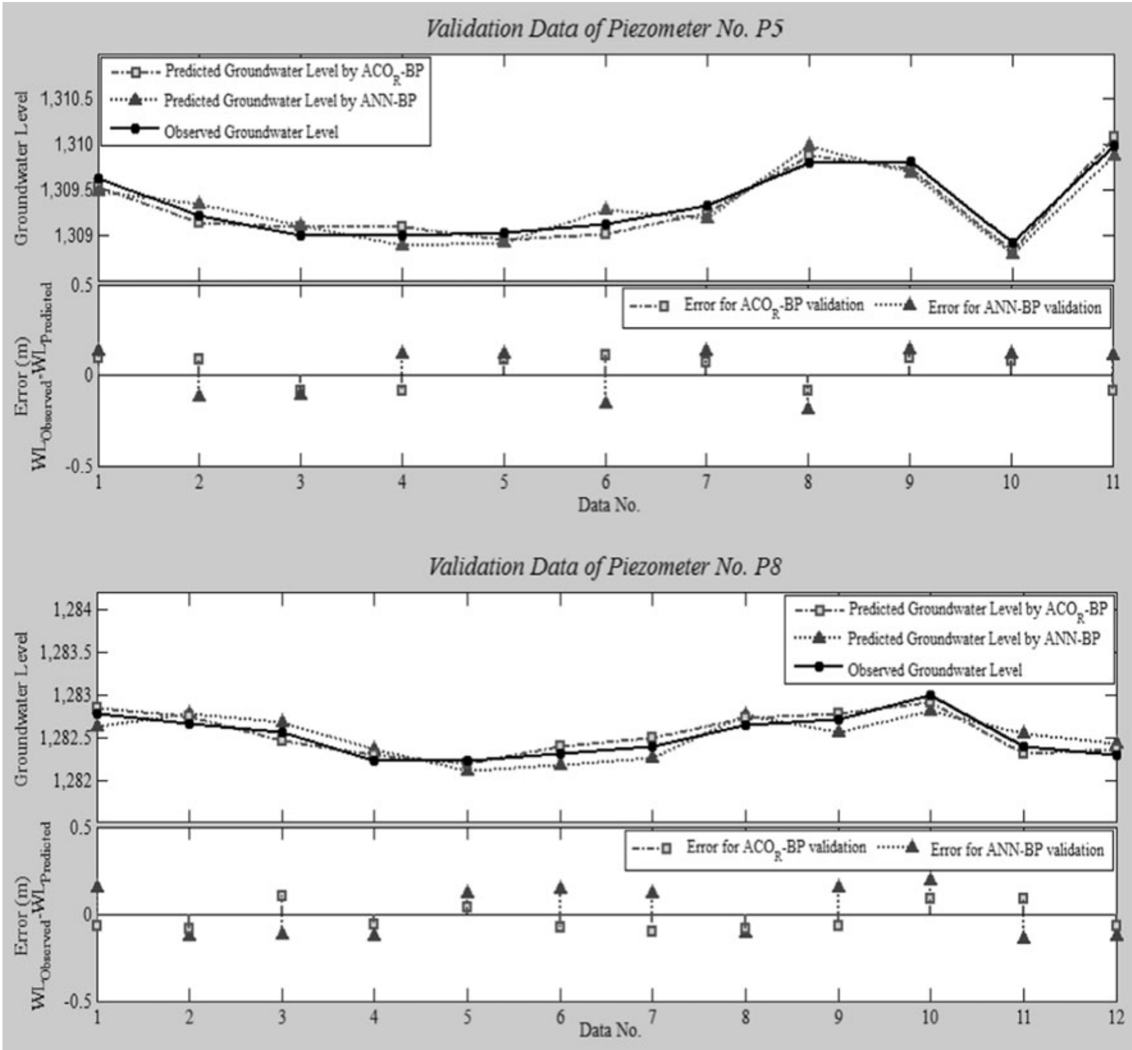


**Fig. 12** Graphical comparison of estimated versus observed groundwater level at two selected piezometers using $ACO_R$-BP and ANN-BP in validation step

The results of prediction at two piezometers (P5 and P8) were illustrated by perfect comparison between the performances of ANN-BP and $ACO_R$-BP models which are presented in Figs. 11 and 12. These image plots have shown a graphical comparison between observed groundwater level and estimated data by using two intelligent models for testing and validation data. As is seen clearly from results, the $ACO_R$-BP model is more successful among the individual models designed (ANN-BP) in this study. This model is faster than ACO stochastic models (Socha 2008). Subsequently, $ACO_R$-BP can be a high prominence in the estimation of groundwater level.

## Conclusion

The study designed an $ACO_R$-BP model to better predict the groundwater level in the complex, heterogeneous, and unconfined aquifer underlying the Shabestar plain, Iran. For this propose, the monthly average of 9-year data including rainfall, temperature, river discharge, annual time series, and evaporation was used as inputs and groundwater levels were considered as the output of the models. The finding and future works are summarized as follows:

1. Because of complex hydrogeological characteristics in the mixing zone, not all AI models are able to accurately predict groundwater levels. In this study, results showed that the $ACO_R$-BP model had better performance than $ACO_R$ and ANN-BP models individually. The simulation results of $ACO_R$-BP model for all piezometers showed that average RMSEs for testing and validation data are 11.29 and 11.83 cm, respectively. Moreover, the average $R^2$ of testing and validation set was more than 90 % for the $ACO_R$-BP model. In the interim, $R^2$ value from test and validation of sum of 15 piezometers for the individual neural network is less than 80 %.

2. The $ACO_R$-BP algorithm can reduce overtraining. This was shown by the difference between training-testing and evaluation being smaller for $ACO_R$-BP than ANN-BP. So, $ACO_R$-BP results are acceptable and ANN-BP results are not suitable for further use of the network in simulation of groundwater level from a coastal aquifer.

3. The results from 30 runs of the models showed that hybrid net has lower distribution in the optimal result. Nevertheless, distributions of results in the piezometers that have high water level changes in each of the two models are considerable.

4. Since most real aquifer systems are heterogeneous and complex, the hybrid $ACO_R$-BP method has a good potential to predict other hydrogeological or hydrochemical parameters. Therefore, in water resources management projects, it can reduce the costs and time required for additional piezometer drilling. Moreover, uncertainty analysis using the $ACO_R$-BP model is also a crucial subject for future research.

## References

Adamowski J, Chan HF (2011) A wavelet neural network conjunction model for groundwater level forecasting. J Hydrol 407(1–4):28–40

Asadian O, Mirzaee AR, Mohajjel M, Hadjialilu B, and Eftekhar Nezhad J, (2007) "Geological quadrangle map of Marand in Iran." Published by: Geological Survey of Iran, map number: 5166.

ASCE Task Committee on Application of Artificial Neural Networks in Hydrology (2000) Artificial neural networks in hydrology, parts I and II. J Hydrol Eng 5(2):115–137

Ashena R, Moghadasi J (2011) Bottom hole pressure estimation using evolved neural networks by real coded ant colony optimization and genetic algorithm. J. Petrol. Sci. Eng. 77:375–385

Behnia N, Rezaeian F (2015) Coupling wavelet transform with time series models to estimate groundwater level. Arab J Geosci 8:1–7

Behzad M, Asghari K, Coppola E Jr (2010) Comparative study of SVMs and ANNs in aquifer water level prediction. J Comput Civ Eng 24(5):408–413

Boucher MA, Perreault L, Anctil F (2009) Tools for the assessment of hydrological ensemble forecasts obtained by neural networks. J. Hydroinform. 11(3–4):297–307

Chau KW (2007) Application of a PSO-based neural network in analysis of outcomes of construction claims. Autom Constr 16(5):642–646

Chebud Y, Melesse A (2011) Operational prediction of groundwater fluctuation in South Florida using sequence based Markovian stochastic model. Water Resour. Manag 25(9):2279–2294

Chen JX, Yu S (2012) Application of ACO-BP algorithm in automobile automatic transmission shift control. Appl Mech Mater 263-266: 553–556

Chen LH, Chen CT, Li DW (2011) Application of integrated back-propagation network and self-organizing map for groundwater level forecasting. J. Water Resour. Plan. Manage. 137(4):352–365

Choubsaz S, Akhoondzadeh M, Saradjian MR (2015) Thermal anomaly detection prior to earthquakes with training artificial neural networks with ant colony optimization. J Hazards Sci 2(2):207–224

Coulibaly P, Baldwin CK (2005) Nonstationary hydrologic time series forecasting using nonlinear dynamic methods. J Hydrol 307:164–174

Coulibaly P, Anctil F, Bobee B (2001a) Multivariate reservoir inflow forecasting using temporal neural networks. J Hydrol Eng 65(9–10):367–376

Coulibaly P, Anctil F, Aravena R, Bobee B (2001b) Artificial neural network modeling of water table depth fluctuation. Water Resour Res 3(4):885–896

Coulibaly P, Bobee B, Anctil F (2001c) Improving extreme hydrologic events forecasting using a new criterion for artificial neural network selection. Hydrol Process 15(8):1533–1536

Daliakopoulos I, Coulibaly P, Tsanis IK (2005) Groundwater level forecasting using artificial neural networks. J Hydrol 309:229–240

Dash NB, Panda SN, Remesan R, Sahoo N (2010) Hybrid neural modeling for groundwater level prediction. Neural Comput. Appl. 19(8): 1251–1263

Datta B, Vennalakanti H, Dhar A (2009) Modeling and control of saltwater intrusion in a coastal aquifer of Andhra Pradesh. India J Hydro-Environ Res 3:148–159

Dawson CW, Wilby RL (2001) Hydrological modeling using artificial neural networks. Prog Phys Geogr 25:80–108

Dogan A, Demirpence H, Cobaner M (2008) Prediction of groundwater levels from lake levels and climate data using ANN approach. Water SA 34:199–205

Fallah-Mehdipour E, Bozorg Haddad O, Marino MA (2013) Prediction and simulation of monthly groundwater levels by genetic programming. J. Hydro-environ. Res. 7:253–260

Giustolisi O, Simeone V (2006) Optimal design of artificial neural networks by a multi-objective strategy: groundwater level predictions. Hydrolog. Sci. J. 51(3):502–523

Giustolisi O, Doglioni A, Savic DA, di Pierro F (2008) An evolutionary multi-objective strategy for the effective management of groundwater resources. Water Resour Res 44(1)

Hornik K, Stinchcombe M, White H (1989) Multilayer feedforward networks are universal approximators. Neural Netw 2:359–366

Hosseini Z, Nakhaei M (2015) Estimation of groundwater level using a hybrid genetic algorithm-neural network. Pollution 1(1):9–21

Jalalkamali A, Jalalkamali N (2011) Groundwater modeling using hybrid of artificial neural network with genetic algorithm. Afr. J. Agricul. Res. 6(26):5775–5784

Jalalkamali A, Sedghi H, Manshouri M (2011) Monthly groundwater level prediction using ANN and neuro-fuzzy models: a case study on Kerman plain. Iran J Hydroinform 13(4):867–876

Kholghi M, Hosseini SM (2009) Comparison of groundwater level estimation using neuro-fuzzy and ordinary kriging. Environ Model Assess 14(6):729–737

Kia A, Ekhlasnia M, Kerdgari M, Maddah H, Alizadeh M (2015) Hybrid neural network performance prediction model for gas assisted gravity drainage recovery method based on the scaling analysis. Petrol. Sci. Technol. 33:1395–1401

Kulluk S (2013) A novel hybrid algorithm combining hunting search with harmony search algorithm for training neural networks. J Oper Res Soc 64(5):748–761

Lallahem S, Mania J (2003a) Evaluation and forecasting of daily groundwater inflow in a small chalky watershed. Hydrol. Process 17(8): 1561–1577

Lallahem S, Mania J (2003b) A non-linear rainfall-runoff model using neural network technique: example in fractured porous media. Math Comput Model 37(9–10):1047–1061

Lallahem S, Mania J, Hani A, Najjar Y (2005) On the use of neural networks to evaluate groundwater levels in fractured media. J Hydrol Eng 307:92–111

Larose DT (2005) Discovering knowledge in data: an introduction to data mining. First Ed. Wiley., New Jersey

Maier HR, Dandy GC (2000) Neural networks for the prediction and forecasting of water resources variables: a review of modeling issues and applications. Environ Model Softw 15(1):101–124

Maier HR, Jain A, Dandy GC, Sudheer KP (2010) Methods used for the development of neural networks for the prediction of water resource variables in river systems: current status and future directions. Environ Model Softw 25(8):891–909

Maiti S, Tiwari RK (2014) A comparative study of artificial neural networks, Bavesian neural networks and adaptive neuro-fuzzy inference system in groundwater level prediction. Environ Earth Sci 71(7):3147–3160

Mavrovouniotis M, Yang S (2014) Training neural networks with ant colony optimization algorithms for pattern classification. Soft Comput 19(6):1511–1522

Mirzavand M, Ghazavi R (2014) A stochastic modeling technique for groundwater level forecasting in an arid environment using time series methods. Water Resour Manag 29:1315–1328

Mirzavand M, Khoshnevisan B, Shamshirband S, Kisi O, Ahmad R, Akib S (2015) Evaluating groundwater level fluctuation by support vector regression and neuro-fuzzy methods: a comparative study , 15 pNat. Hazards

Moosavi V, Vafakhah M, Shirmohammadi B, Behnia N (2013) A Wavelet-ANFIS hybrid model for groundwater level forecasting for different prediction periods. Water Resour Manag 27(5):1301–1321

Moosavi V, Vafakhah M, Shirmohammadi B, Ranjbar M (2014) Optimization of Wavelet-ANFIS and Wavelet-ANN hybrid models by Taguchi method for groundwater level forecasting. Arab J Sci Eng 39(3):1785–1796

Nadiri AA, Fijani E, Tsai F, Asghari Moghaddam A (2013) Supervised committee machine with artificial intelligence for prediction of fluoride concentration. J. Hydroinform. 15:1474–1490

Nakhaei M, Saberi Naser A (2012) A combined Wavelet-Artificial neural network model and its application to the prediction of groundwater level fluctuations. J. Geope. 2(2):77–91

Nourani V, Ejlali RG, (2012) Quantity and quality modeling of groundwater by conjugation of ANN and co-kriging approaches. (In P. Nayak, (Ed.), Water resources management and modeling, E-Publishing, InTech. pp. 287–310).

Nourani V, Ejlali RG, Alami MT (2011) Spatiotemporal groundwater level forecasting in coastal aquifers by hybrid artificial neural network-geostatistics model: a case study. Environ Eng Sci 28(3): 217–228

Nourani V, Hosseini Baghanam A, Daneshvar Vousoughi F, Alami MT (2012) Classification of groundwater level data using SOM to develop ANN-based forecasting model. Int. J. Soft Co. Eng. (IJSCE) 2(1):464–469

Nourani V, Moghaddam AA, Nadiri A (2008) An ANN-based model for spatiotemporal groundwater level forecasting. Hydrol Process 22: 5054–5066

Raghavendra NS, Deka PC (2015) Forecasting monthly groundwater level fluctuations in coastal aquifers using hybrid wavelet packet-support vector regression. Cogent Eng 2(1):1–22

Safarvand D, Alizadeh M, Samipour Giri M, Jafarnejad M (2015) Exergy analysis of NGL recovery plant using a hybrid $ACO_R$-BP neural network modeling: a case study. Asia Pac J Chem Eng 10:133–153

Sahoo S, Jha MK (2013) Groundwater-level prediction using multiple linear regression and artificial neural network techniques: a comparative assessment. Hydrogeol J 21(8):1865–1887

Shiri J, Kisi O (2011) Comparison of genetic programming with neuro-fuzzy systems for predicting short-term water table depth fluctuations. Computers Geosci 51:108–117

Shiri J, Kisi O, Yoon H, Lee KK, Nazemi AH (2013) Predicting groundwater level fluctuations with meteorological effect implications—a comparative study among soft computing techniques. Comput Geosci 56:32–44

Socha K (2008) Ant colony optimization for continuous and mixed-variable domains. Universite Libre de Bruxelles, Belgium, PhD dissertation

Socha K, Blum C (2007) Hybrid ant algorithms applied to feed-forward neural network training: an application to medical pattern classification. NCA 16(3):235–248

Socha K, Dorigo M (2008) Ant colony optimization for continuous domains. Eur J Oper Res 185(3):1155–1173

Sreekanth PD, Geethanjali N, Sreedevi PD, Ahmad S, Ravi Kumar N, Kamala Jayanthi PD (2009) Forecasting groundwater level using artificial neural networks. Curr Sci India 96(7):933–939

Tabatabaei SME, Kadkhodaie-Ilkhchi A, Hosseini Z, Asghari Moghaddam A (2015) A hybrid stochastic-gradient optimization to estimating total organic carbon from petrophysical data: a case study from the Ahwaz oilfield, SW Iran. J. Petrol. Sci. Eng. 127:35–43

Taormina R, Chau K, Sethi R (2012) Artificial neural network simulation of hourly groundwater levels in a coastal aquifer system of the Venice lagoon. Eng Appl Artif Intell 25(8):1670–1676

Triana E, Labadie JW, Gates TK, Anderson CW (2010) Neural network approach to stream-aquifer modeling for improved river basin management. J Hydrol 391:235–247

Tsanis IK, Coulibaly P, Daliakopoulos IN (2008) Improving groundwater level forecasting with a feedforward neural network and linearly regressed projected precipitation. J. Hydroinform. 10(4):317–330

Wang LY, Zhao WG (2010) Forecasting groundwater level based on wavelet network model combined with genetic algorithm. Adv Mater Res 113-116:195–198

Yang Q, Hou Z, Wang Y, Zhao Y, Delgado J (2014) A comparative study of shallow groundwater level simulation with WA-ANN and ITS model in a coastal island of south China. Arab J Geosci 7:1–11

Yang ZP, Lu WX, Long YQ, Li P (2009) Application and comparison of two prediction models for groundwater levels: a case study in Western Jilin Province. China J Arid Environ 73:487–492

Ying Z, Wenxi L, Haibo C, Jiannan L (2014) Comparison of three forecasting models for groundwater levels: a case study in the semiarid area of west Jilin Province, China. Journal of Water Supply: Res. TechnoAQUA 63(8):671–683